Desalination and Water Treatment
www.deswater.com

doi: 10.5004/dwt.2021.27596

235 (2021) 272–282
September

A brief study of adsorption of Congo red dye over sawdust of *Cedrus deodara*

Ilyas Muneer[a], Tariq Javed[a,*], Aysha Abdul Majeed[b], Hafiz Tariq Masood[c]

[a]*Department of Chemistry, University of Sahiwal, Sahiwal, Pakistan, Tel. +92-3016153258; email: ilyasmuneer70@gmail.com (I. Muneer), Tel. +92 3360916597; email; mtariq@uosahiwal.edu.pk (T. Javed)*
[b]*Department of Zoology, Government Associate College for Women Jhelum, Pakistan, email: ayeshagcwjhelum@gmail.com*
[c]*Department of Physics, University of Sahiwal, Sahiwal, Pakistan, email: tariq@uosahiwal.edu.pk*

Received 8 June 2020; Accepted 7 July 2021

ABSTRACT

Adsorptive removal of Congo red dye from aqueous media has been carried out by using sawdust of *Cedrus deodara* saw as an efficient adsorbent by evaluating different parameters such as adsorbent dosage, contact time, pH, initial dye concentration, and temperature at constant shaking time of five minutes by using a Benchtop orbital shaker to homogenize adsorption medium that develops more attractive forces between *C. deodara* saw and dye molecules lead to higher adsorption values. The *C. deodara* saw surface morphology was monitored by Fourier transform infra-red spectroscopy and scanning electron microscopy analysis. The adsorption experimental data was studied by applying the Langmuir, Freundlich, and Dubinin–Radushkevich isothermal models, and data was well obeyed by D–R isotherm based on R^2 and SSE (0.996, 0.004) values. The kinetics of the adsorption process was investigated by pseudo-first-order, pseudo-second-order, liquid film, and intra-particle diffusion models. Kinetics indicated that the pseudo-second-order model behaves as the most favored model with a 1.0 R^2 value but the adsorption process can also be explained with the help of more than one kinetic mechanism (liquid film and intra-particle models). The values for thermodynamic parameters such as ΔG, ΔS, and ΔH were indicating the spontaneity and endothermic nature of the reaction. The applicability of the developed procedure was studied in tap water with 94% removal of Congo red dye. These results suggested that sawdust of *C. deodara* could be used as a low-cost alternative waste material adsorbent for synthetic dye removal.

Keywords: Adsorption; *Cedrus deodara*; Congo red; Thermodynamics

1. Introduction

Water is a major component of the environment and has dynamic importance in maintaining life on earth. But with the increasing population of human beings on the earth, the world has made much more progress in the field of industries like textile, paper, leather, foodstuff, etc. [1] to improve the lifestyle of human beings. These kinds of industries are using many organic dyes like Congo-red and crystal violet dyes as raw materials for coloring purposes as an addition to the major raw material which is used for pre-coloring in manufacturing processes and storage purposes and producing a remarkable amount of waste material including many organic dyes (Congo red, crystal violet, and vat dyes) heavy metals and waste remains. By adding such waste materials directly to the resources of water like sea, rivers, lakes, and ponds without being treated they are making water unhealthy to use for human beings as well injurious to the aquatic life [2].

Most of the dyes are organic-azo dyes that are used for coloring purposes and about 53% of these azo dyes are registered as non-biodegradable [3]. Around 2% of dyes are released during the formation process of dyes [4] and about 10%–15% during dyeing the products of industries [5]. A small amount of these dyes can impart a grace shadow to water [6] and will disturb the aquatic ecosystem by

* Corresponding author.

disturbing the photosynthesis in water resources [7]. Most of these dyes (Congo red) are carcinogenic [8], mutagenic, and cause many additional problems to humans in the form of diseases so, they must be removed from the environment. There is a need to remove Congo red dye because it is highly toxic and carcinogenic in nature and has drastic effects on human health [9].

Several techniques have been developed and used so far including oxidation, ion exchange method, floatation process, membrane filtration, and solvent extraction methods [10–12] for competing for this challenge but the most important one is the adsorption techniques because of its ease in operation and its economical suitability [13]. In the adsorption process, we use the adsorbents (the waste materials which having no financial importance at all) which have the ability to remove a large variety of waste material from water including dyes and heavy metals [14] some of these adsorbents are *Solanum tuberosum* waste [43], *Pisum sativum* waste [43], rice husk ash [44], white dragon fruit peel [16]. Moreover, the use of such type of waste material is an eco-friendly action [17]. Current studies primarily now focusing on the searching of adsorbents with economically low valuable and easily accessible with high fitness to adsorb the waste materials from aqueous solutions [18]. The agricultural waste material can be used for this purpose efficiently [19,20].

In this study, the adsorption capacity of sawdust of *C. deodara* to remove the Congo red dye from aqueous media was investigated. Several factors including contact time, temperature, the weight of adsorbent, initial concentration of dye, and pH were examined during this work which has a great influence on % age removal of Congo red dye over sawdust of *C. deodara*. It is worth mentioning that no work has been presented yet on the adsorption of Congo red dye by using sawdust of *C. deodara* in the following reporting department.

2. Materials and methods

2.1. Preparation of reagents

The 1,000 mg L^{-1} stock solution of Congo red dye (Direct Red 28, C.I.22120, azo dye) was prepared in a 1,000 mL measuring flask by the addition of 1.0 g of Congo red dye in the measuring flask then diluted with double distilled water up to the mark. The stock solution was then stored carefully. pH solutions were prepared by using natural acid and base (H_2SO_4 and KOH). Further successive dilutions were made with the help of an accurately prepared stock solution of Congo red dye in double-distilled water.

2.2. Collection of sawdust of C. deodara

The sawdust of *C. deodara* was collected from Mian Channu (Province Punjab, Pakistan) and further ground to get the fine powdered form. Then, it was sieved to get different sizes of particles of 100, 200, and 500 μm. These different particles sizes of adsorbent were stored in different labeled plastic airtight containers to avoid further moisture contact. The 100 μm sized particles of *Cedrus deodara* saw were used for the corresponding study due to the availability of large surface area and more active sites for adsorption of Congo red dye.

2.3. Batch adsorption studies

Batch adsorption experiments were performed to evaluate the different factor which controls the adsorption process such as range of contact time (min), the weight of adsorbent (g), pH, initial concentration of dye (mg L^{-1}) solution and temperature (°C) and each experiment was performed for three times to reduce random errors. The concentration of dye used for the evaluation of factors was 100 mg L^{-1}. All the experiments were performed with the addition of an appropriate amount of adsorbent in 10 mL of dye solution which was freshly prepared by the diluting stock solution. After shaking the mixture for provided time durations the adsorbent was separated by applying centrifugation and filtration processes. The extent of dye adsorption on the adsorbent surface was evaluated by the absorption spectrophotometer (Visible spectrophotometer-721). Before checking the absorption, a blank sample was run each time. All the experiments were performed at room temperature except the specific experiment of temperature evaluation. The percentage adsorption was calculated by the given expression:

$$\%\ \text{age adsorption} = \left(\frac{A_i - A_f}{A_i}\right) \times 100 \tag{1}$$

where A_i and A_f are the initial and final values of absorbance, respectively.

2.4. Characterization

2.4.1. Fourier transform infra-red spectroscopy

Fourier transform infra-red spectroscopy (FT-IR) spectra were recorded by using attenuated total reflectance (ATR) with an FT-IR spectrometer for the characterization of functional groups present on the adsorbent surface [19]. *C. deodara* saw functional group morphology was examined before and after adsorption of Congo red dye.

2.4.2. Scanning electron microscope

The technique of scanning electron microscope (SEM) was used to characterize the surface morphology of the *C. deodara* saw surface and for evaluation of the basic physical properties of the adsorbent. It was useful in determining the size of grooves, shape, and porosity of adsorbent [21]. The SEM technique was applied on two samples native and loaded of adsorbent, magnification of 800x was used.

3. Results and discussion

3.1. Fourier transform infra-red spectroscopy

The FT-IR spectra for the *C. deodara* sawdust were obtained from two samples: without and with adsorption of Congo red dye represents the relation between percentage transmittance and wave number (cm^{-1}) are shown in Fig. 1a and b, respectively. The functional groups which were mainly involved in the adsorption of Congo red dye over *C. deodara* saw were C=O, –COOH, R–OH, Ar–NH_2, and R–NH_2 with –OH groups which were strongly consumed and regained in the adsorption mechanism. The wide and intense

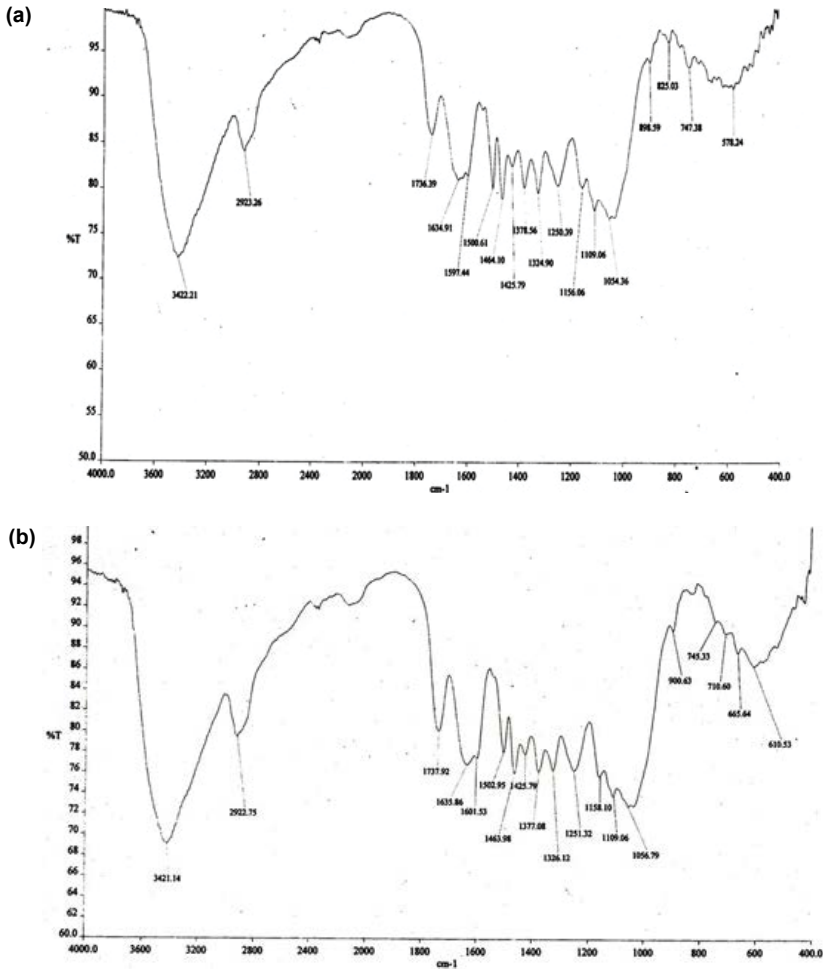

Fig. 1. FT-IR of *Cedrus* deodara saw (a) before and (b) after adsorption of Congo red dye.

adsorption peaks found at 3,422.215 and 3,421.142 cm^{-1} are due to the stretching vibrations of –OH (hydroxyl) groups and these peaks are visible at both spectra before and after adsorption of dye, moreover, they exhibits the availability of positively charged surface that attracts Congo red molecules during adsorption. The bands at 2,923 and 898 cm^{-1} could be assigned to the stretching of the –CH group and the presence of alkanes and alkenes, respectively. The climax at 1,634.91 and 1,737.92 cm^{-1} are assigned to the stretching of carbonyl groups (carboxylic acids). The peak of spectra presents at 1,054 and 1,109 cm^{-1} are characteristics of stretching of C–O and C–N groups (Amines, Imines). The peaks present at 1,250 cm^{-1} are due to stretching vibrations of C=O groups and at 1,464, 1,500, and 1,597 cm^{-1}, and the bending vibrations present at 747–898 cm^{-1} are due to the C=C of alkyl groups stretching in rings which may be benzene, cyclo-hexenes [21]. The functional groups of Congo red dye after adsorption were $–NH_2$ and $–SO_3$ which involved in adsorption and were observed in FT-IR spectral analysis.

3.2. Scanning electron microscopy

SEM was used as a basic technique for the characterization of porosity and shape of grooves present in an adsorbent surface before and after adsorption. The micrographs for the *C. deodara* before and after adsorption of Congo red dye over its surface are shown in Fig. 2a and b, respectively. Fig. 2a represents the presence of a number of pore sites available in *C. deodara* saw due to which there was a qualitative possibility of dye to be trapped inside the pores. Fig. 2b exhibits the dark spots, which were very obvious signs of adsorption of dye into the pores of the adsorbent [21]. There was a major difference between before and after adsorption of dye molecules on the *C. deodara* saw surface as before adsorption adsorbent surface contained grooves and lumps of about 20 μm in size while after dye adsorption many sites where vanished due to pore filling of *C. deodara* saw and Fig. 2b shows 50 μm grooves size that could be the evidence of adsorption of dye molecules, respectively.

3.3. Effect of adsorption controlling parameters

The parameters that control the adsorption process are contact time (min), initial concentration of dye (mg L^{-1}), amount of adsorbent (g), pH, and temperature (°C) were investigated in detail and their results are discussed below.

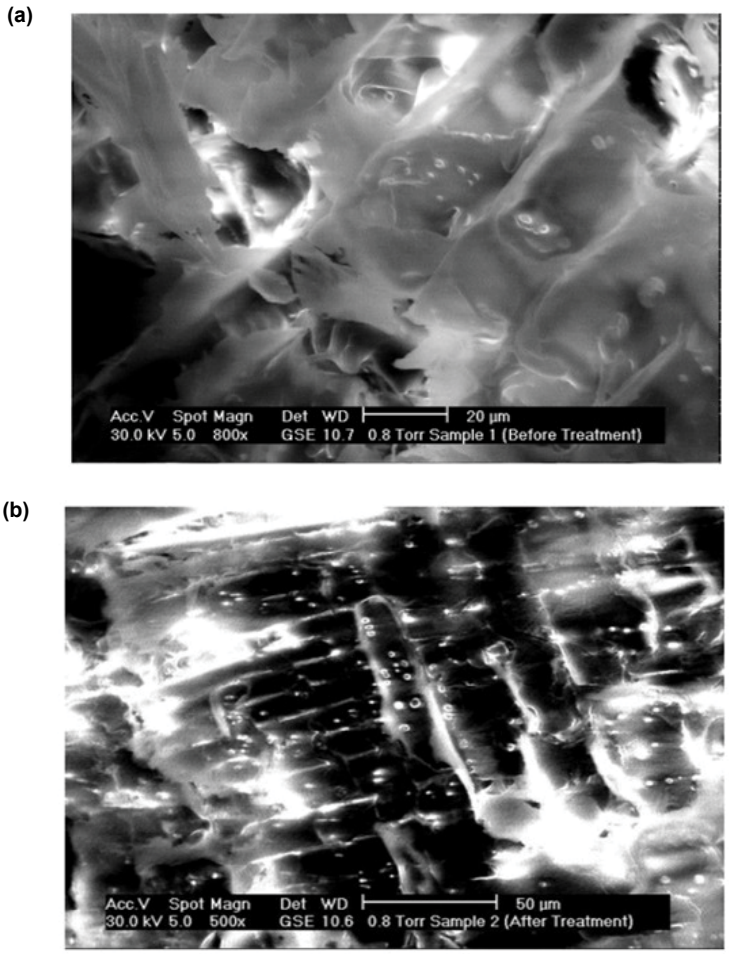

Fig. 2. SEM of *Cedrus* deodara saw dust (a) before and (b) after adsorption of Congo red dye.

3.3.1. Effect of the weight of adsorbent (g)

The effect of adsorbent dosage (*g*) was examined by varying the weight of adsorbent ranging from 0.1 to 1.3 g at 100 mg L^{-1} initial dye concentration, 20 min contact time, and 7.0 pH at room temperature, respectively (Fig. 3). Fig. 3 represents that there was an increase in percentage removal of dye firstly and then constant adsorption was observed after 1.1 g weight of *C. deodara* saw. The increase in adsorption firstly was due to increase in surface area of adsorbent with an increasing amount of adsorbent but further from 1.1 g, there was a constant value of adsorption, irrespective of this, that the surface area was increasing with the increase in weight but the volume and concentration of dye were constant due to which the percentage adsorption becomes constant. Fig. 3 explains the effect of adsorbent dosage on percentage removal of dye from aqueous solution briefly. The percentage removal was 68%, 71%, 84%, 88%, and 92% for adsorbent weights 0.1, 0.3, 0.5, 0.7 and 0.9 g, respectively. The maximum 94% adsorption was reported at the highest *C. deodara* saw dosage of 1.1 g because with the increase of weight of adsorbent, there was an increase in the number of sites available for the constant concentration of dye solution. Similar results for Congo red were reported for phoenix D. seeds [22].

3.3.2. Effect of pH

The effect of pH on the removal of Congo red dye was observed by varying the pH from 1 to 12 pH at 100 mg L^{-1} initial dye concentration, 20 min contact time, and room temperature (20°C). The pH of solutions was maintained by using mineral acid and base (H_2SO_4 and KOH). The percentage dye removal was decreasing for the first three values from 1–3 pH and then was an increase in percentage removal till 7.0 pH at which maximum adsorption of about 94% takes place. Again from 8 to 12 values of pH, there was a decrease in percentage removal. Fig. 4 explains the effect of pH values on the removal of Congo red dye by sawdust of *C. deodara* as an adsorbent. At pH 1.0, the surface of *C. deodara* saw exhibits negatively charged surface and $–SO_3Na$ functional groups of dye show involvement in adsorption that's why 82% adsorption of Congo red takes place. While at pH 10 adsorbent surface shows the availability of positive charges by releasing –OH and $–NH_2$ groups of Congo red dye involved in adsorption. But at pH 7.0, there is a possibility of the presence of both positive and negative characters of *C. deodara* saw a surface that's why maximum adsorption of 94% was monitored. The maximum adsorption of Congo red at pH 7 was also reported for zeolitic imidazolate, vermicompost dried-biochar adsorbents [23], and aniline propylsilica xerogel [24].

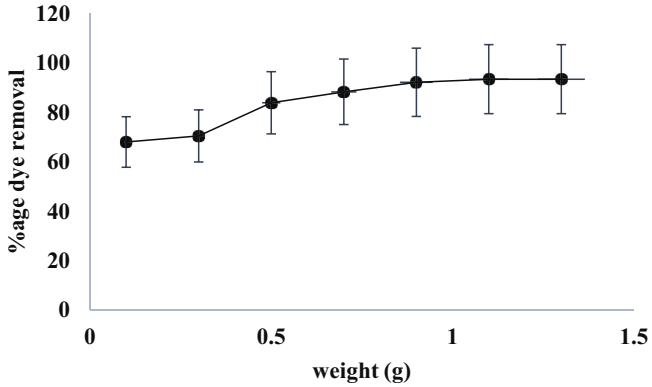

Fig. 3. Effect of weight of adsorbent (100 mg/L concentration, 20 min contact time at pH 7.0).

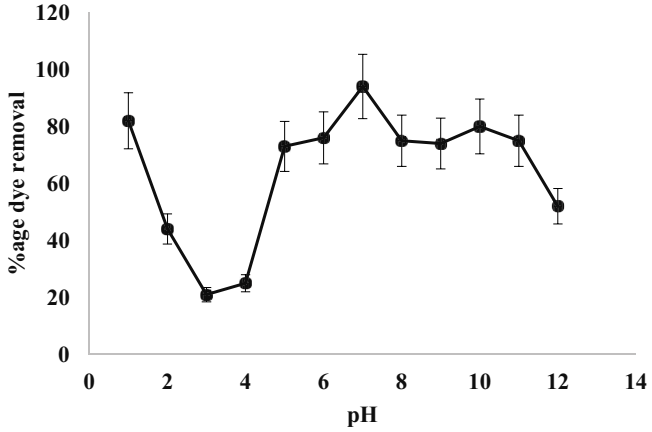

Fig. 4. Effect of pH (100 mg L^{-1} initial dye concentration, 20 min contact time at room temperature).

3.3.3. Effect of contact time (min)

The effect of shaking time on percentage removal of Congo red dye was investigated by varying the time of duration from 5 to 120 min and other parameters were 100 mg L^{-1} initial dye concentrations, pH of 7 at room temperature. Fig. 5 explains the impact of contact time on the removal of Congo red dye at the constant amount (g) of sawdust of *C. deodara*. Firstly, the removal percentage was increasing at a high rate till 50 min of contact time but afterward, irrespective of this, that the percentage removal was increasing with time but there was a decrease in the rate of adsorption of dye over the surface of the adsorbent because during the time duration of 5–50 min due to the presence of more sites on the adsorbent surface for the dye molecules the rate of adsorption was more but with the passage of time the space over the surface was lessened due to which the rate of adsorption of dye was not much increase after 50 min of contact time or seems to be constant. The maximum adsorption took place at the time of 120 min and it was 86% was showing similar behavior on comparison along with percentage dye removal by increasing time from 5 to 120 min with respect to the corresponding adsorbent surface. The comparison between and temperature is also given in Fig. 5.

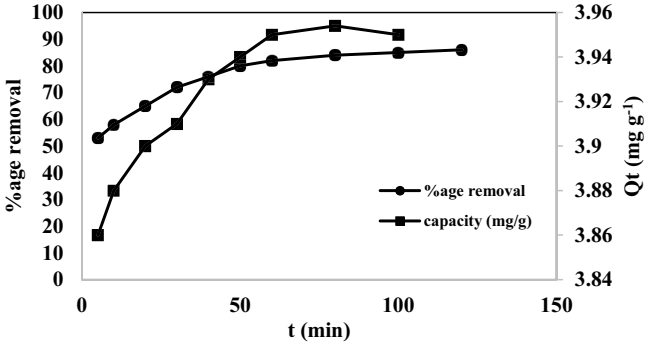

Fig. 5. Effect of contact time on percentage dye removal and Q_t (100 mg L^{-1} initial dye concentration, pH 7.0 at room temperature 20°C).

3.3.4. Effect of the initial concentration of dye

The initial concentration of dye is very important for the adsorption process. Fig. 6 shows the effect of initial concentration on percentage removal was investigated by varying the initial dye concentration from 5 to 100 mg L^{-1} while all other factors were constant. At a lower concentration of 5 mg L^{-1}, the percentage adsorption was maximum of 99% and at a higher concentration of 100 mg L^{-1}, the adsorption was minimum which is reported as 72% at room temperature. More sites were available at the surface of adsorbent for a lower concentration of dye while at a higher concentration less number of binding sites were available for the dye molecules due to which at lower concentration percentage removal was maximum and vice versa. A decrease in percentage removal with the increase in initial concentration of Congo red dye for *Phragmites australis* adsorbent was also reported [25]. But at a higher concentration of Congo red 72% dye removal represents the good chemistry between *C. deodara* saw and adsorbate molecules which is of major concern.

3.3.5. Effect of temperature (K)

The effect of temperature on adsorption of Congo red dye over sawdust of *C. deodara* was studied by varying the range of temperature from 273 to 343 K and by keeping all other operative factors as 100 mg L^{-1} initial dye concentration, 20 min contact time at pH of about 7.0. There was an increase in adsorption percentage with an increase in temperature was revealing that there was a direct relationship between temperature and percentage dye removal. Maximum adsorption takes place at a higher temperature. The percentage removal was varied from 12% to 85% with a temperature range of 273 to 343 K. The results are graphically explained in Fig. 7. The increase in the adsorption process with an increase in temperature may be due to the increase of the rate of slow steps of adsorption or may be due to an increase in binding sites on the surface of the adsorbent. Similar effects for adsorption of Congo red dye over the N,O-carboxymethylchitosan, and montmorillonite nanocomposite [26] were studied. Exhibit similar behavior on comparison with percentage dye removal by increasing temperature from

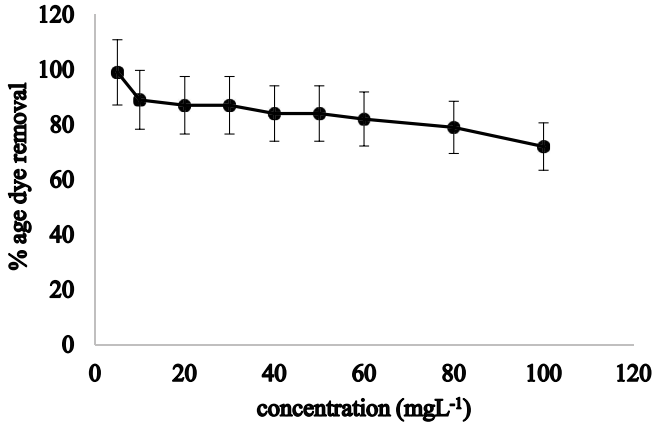

Fig. 6. Effect of initial concentration (0.3 g of adsorbent, pH 7 at room temperature).

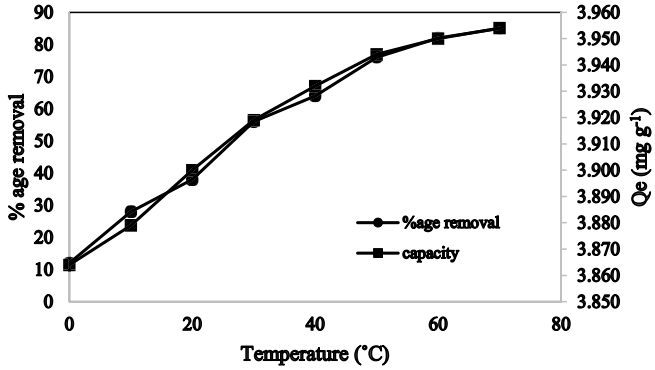

Fig. 7. Effect of temperature on percentage removal and Q_e (100 mg L^{-1} initial dye concentration, 20 min contact time at pH 7.0).

273 to 343 K with respect to a corresponding adsorbent surface (Fig. 7).

3.4. Kinetics of adsorption process

Time depended data was applied to study the kinetic mechanism followed by Congo red dye over *C. deodara* saw.

3.4.1. Pseudo-first-order reaction

The kinetic equation of pseudo-first-order reactions was first given by Lagergren in 1898 and demonstration with the help of the following equation [27]:

$$\log\left(Q_e - Q_t\right) = \log Q_e - \left(\frac{k_1}{2.303}\right) \times t \tag{2}$$

The concentration of dye at equilibrium position is Q_e, the concentration of dye at specific time 't' is Q_t and k_1 is the constant used for rate per unit time of first-order kinetic model. By drawing a plot between $\log(Q_e - Q_e)$ against time t a straight line with intercept $\log Q_e$ and slope k_1 was obtained [28] given in Fig. 8. The values for k_1 (min^{-1}) and Q_e (mg g^{-1}) were determined by the slope and intercept and are given in Table 1. The regression value of correlation factor R^2 for the pseudo-first-order kinetics was less than the pseudo-second-order kinetic but there was not a big difference between calculated (0.137) and experimental (0.14) values of Q_e for pseudo-first-order kinetics which reveals that the adsorption of Congo red over *C. deodara* saw is much followed by the pseudo-first-order kinetics mechanism as well as the second order.

3.4.2. Pseudo-second-order kinetics

The kinetic expression for the pseudo-second-order reaction can be written as follows [27]:

$$\frac{t}{Q_t} = \left(\frac{1}{k_2 Q_e^2}\right) + \left(\frac{t}{Q_e}\right) \tag{3}$$

where t, Q_t, and Q_e are time, amount of dye adsorbed at time t, and amount of dye adsorbed at equilibrium contact time. By plotting a graph between t/Q_t and time t, we get a straight line with slope $1/Q_e$ and intercept $1/h$. Where 'h' equals to $1/k_2 Q_e^2$ [29] as given in Fig. 8. The values for k_2 (g mg^{-1} min^{-1}) and Q_e (mg g^{-1}) were calculated by the slope and intercept and are placed in Table 1. The regression or correlation value R^2 for pseudo-second-order kinetics was 1.0 which is greater than the regression value of pseudo-first-order kinetics (0.989). Moreover, the calculated value (3.957) of Q_e by the pseudo-second-order kinetics was closer to the experimental value (3.966) of Q_e. So, it was concluded that the experimental data of Congo red adsorption over *C. deodara* saw follows the pseudo-second-order kinetics is well manner.

3.4.3. Intra-particle diffusion model

The simplified form of the equation for the intra-particle diffusion model can be written as follows [30]:

$$Q_t = k_p t^{\frac{1}{2}} \tag{4}$$

where k_p is the rate constant and it can be calculated by the linear regression value of the data of experiment which was plotted as Q_t vs. $t^{1/2}$. The plot should be passing through the origin with a straight line when about 40% of the equilibrium amount of dye is adsorbed over the surface of the adsorbent. But the plot obtained by the data is not linear at all, as shown in Fig. 9a. It means that this model is not only governing the adsorption procedure. Besides of all the lower values of the coefficient of correlation for the intra-particle diffusion model suggested that the diffusion model is not sufficient for explaining the mechanism of adsorption. To be very clear with results that the adsorption of Congo red dye over sawdust of *C. deodara* cannot be represented by the single adsorption kinetic mechanism.

3.4.4. Liquid film diffusion model

The liquid film diffusion or Reichenberg model can be expressed as [31]:

$$\ln\left(\frac{1-Q_t}{Q_e}\right) = -K_{fd} \times t \tag{5}$$

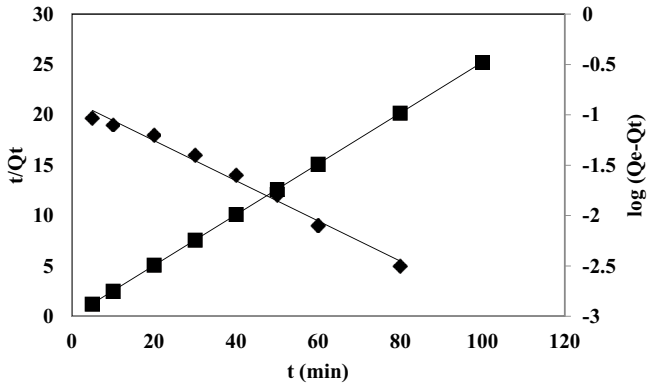

Fig. 8. Pseudo-first- and second-order kinetics.

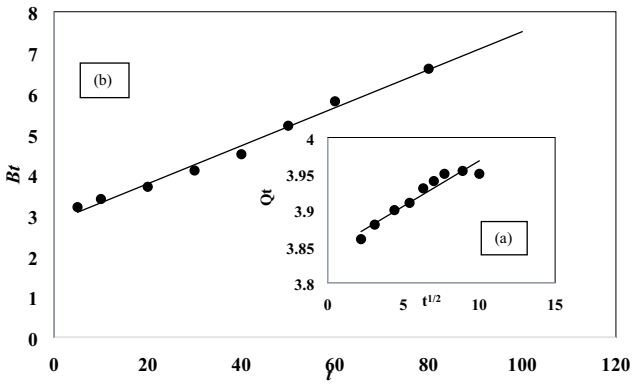

Fig. 9. Intra-particle diffusion model (a) and liquid film model (b).

Table 1
Parameters of kinetic models

Kinetic equation	Parameters		R^2
Pseudo-first-order	Q_e (mg g^{-1}) 0.14	K_1 (min^{-1}) 0.047	0.9892
Pseudo-second-order	Q_e (mg g^{-1}) 3.966	K_2 (g mg^{-1} min^{-1}) 1.061	1

$Q_{e\,(exp)}$ is 3.957 which is closer to pseudo-second-order kinetics.

This equation can also be simplified as follows.

$$\beta_t = -0.4977 - \ln\left(1 - \frac{Q_t}{Q_e}\right) \tag{6}$$

where K_{fd} is the rate constant for the liquid film diffusion model. The plot between β_t vs. time t should be a straight-line graph. Q_e is an amount of dye adsorbed in mg g^{-1} over the surface of adsorbent at equilibrium time and Q_t is the amount of dye adsorbed in mg g^{-1} at a given time t. This model can only be applicable if a straight line of graph passes through the origin and from Fig. 9b, it is clear that the line was unable to pass through the origin which limits the applicability of this model on the adsorption mechanism of this Congo red dye over *C. deodara* saw. So, it can be easily concluded that the present adsorption phenomenon cannot be explained by single adsorption kinetics.

3.5. Adsorption isotherms

For the application of adsorption process on commercial and industrial scale, the quantification of adsorption data and procedure is very necessary. The equilibrium of adsorption was used as an important tool for analyzing and formatting the adsorption process because it provides all important, necessary, and informational data about the physiochemical nature of adsorbent for predicting its applicability at different scales. For this purpose, the data of adsorption of Congo red dye over the surface of sawdust of *C. deodara* related to the dye concentration parameter was subjected and analyzed by different isothermal models including Langmuir, Freundlich, and Dubinin–Radushkevich isotherms. And the comparison of adsorption capacity (mg g^{-1}) of different adsorbents with present studies is given in Table 3.

3.5.1. Langmuir adsorption isotherm

The Langmuir adsorption isotherm has been used by various researchers in different systems. This model explains the homogeneity of the adsorbing surface with no interactions between adsorbed species and adsorbent, at equilibrium conditions. The following equation is the linearized form of Langmuir [32]:

$$\frac{C_e}{C_{ads}} = \frac{1}{\left(Q_m K_L + C_e / Q_m\right)} \tag{7}$$

In this equation, Q_m is a constant known as monolayer adsorption capacity (mg g^{-1}), K_L or some time written as "*b*" (dm^3 mol^{-1}) is a constant related to the energy of the adsorption. Generally, constant Q_m and K_L describe the functions of adsorbate: mainly pH, ionic medium, and ionic strength. The value of Q_m was calculated with the help of the linearized form of Langmuir adsorption isotherm by plotting a graph between C_e/C_{ads} (g L^{-1}) vs. C_e (mol L^{-1}) as shown in Fig. 10(a). The maximum value for R^2 was considered as the best fit model to explain the isothermal behavior of the adsorption process. All determined constants for Langmuir adsorption isotherm are given in Table 2 with SSE. To compare the fitness of different models of isotherms the value of R^2 for linearized form and SSE may be calculated as follows [31]:

$$R^2 = \frac{\sum\left(C_{ads,cal} - C_{ads,exp}\right)^2}{\sum\left(C_{ads,cal} - C_{ads,exp}\right)^2 - \sum\left(C_{ads,cal} - C_{ads,cal}\right)^2} \tag{8}$$

$$SSE = \sum_{i=1}^{N}\left(C_{exp} - C_{cal}\right)^2 \tag{9}$$

where $C_{ads,cal}$ is the calculated value for the amount of dye adsorb (mol g^{-1}), $C_{ads,exp}$ is an experimental value for the amount of dye adsorb at the surface of adsorbent (mol g^{-1}).

As an essential feature of Langmuir isotherm is a constant dimensionless term known as R_L parameter and it is used to find either the adsorption system is favorable or unfavorable and it is represented as follows [34]:

$$R_L = \frac{1}{\left(1+bC_0\right)} \tag{10}$$

where "*b*" can also be written as K_L. C_0 is the initial concentration in mol L^{-1}. The value of R_L may predict the results as follows [33].

- If R_L is in between 0 and 1, then adsorption will be favorable
- If R_L is greater than 1 adsorption will be unfavorable.
- If R_L is equals to 1, then linear adsorption will occur.
- If R_L is equals to 1, then irreversible adsorption will occur.

The calculated value for R_L given in Table 2, 0.981 which was in between 0 and 1, so the adsorption process for Congo red dye over sawdust is said to be more favorable. In Fig. 10(a) relation between C_e (mol L^{-1}) and Q_e (mg g^{-1}) is also given. There was a direct relation between C_e (mol L^{-1}) and Q_e (mg g^{-1}). With the increase of C_e (mol L^{-1}) the Q_e (mg g^{-1}) was also increased.

Table 2
Parameters of isotherms

Isotherm model	Parameters	R^2	SSE	
Freundlich	1/*n* 0.9079	K_f (m mol g^{-1}) 66,044	0.992	0.057
Langmuir	Q_m (mg g^{-1}) 182.5	*b* (dm^3 mol^{-1}) 137,072	0.8535	0.011
D–R	β (kJ^{-2} mol^{-2}) 0.0054	E_s (kJ mol^{-1}) 7.44	0.9964	0.004

3.5.2. Freundlich adsorption isotherm

Freundlich adsorption isothermal expression was proposed by the H.F. Freundlich which can be written as follows [34]:

$$C_{\text{ads}} = K_f C^{\frac{1}{n}} \tag{11}$$

The linearized form of the above equation can be represented as follows [34]:

$$\log C_{\text{ads}} = \log K_f + \frac{1}{n\left(\log C_e\right)} \tag{12}$$

where C_e is the concentration of dye adsorbed at equilibrium (mol L^{-1}) and C_{ads} termed as the concentration of dye adsorbed per unit mass of adsorbent (mol g^{-1}). K_f and "*n*" are the Freundlich constants that indicate the adsorption capacity and intensity, respectively. If the experimental data gave the best fitness over the Freundlich isotherm, it reveals that multilayer adsorption will occur, and the amount of dye adsorb over *C. deodara* saw surface will have no limit. The linear form of Freundlich adsorption isotherm is given in the following Fig. 10b and obtained parameters of the Langmuir model are given in Table 2.

3.5.3. Dubinin–Radushkevich adsorption isotherm (D–R)

The non-linearized form of D–R isothermal expression can be expressed as [31]:

$$C_{\text{ads}} = C_m \exp\left(-\beta\varepsilon^2\right) \tag{13}$$

where C_{ads} is the concentration or amount of Congo red dye adsorb over the surface of the adsorbent. C_m (mol g^{-1}) is the maximum amount of Congo red dye adsorbed over the sawdust, β is the constant related to the energy of the adsorption process and ε is also a constant called Polyanyi potential and can be expressed as [35]:

$$\varepsilon = RT\ln\left(1+\frac{1}{C_e}\right) \tag{14}$$

Table 3
Comparison of adsorption capacity of different adsorbents to remove Congo red dye

Adsorbent	Equilibrium concentration (mg L^{-1})	Adsorption capacity (mg g^{-1})	Equilibrium time (min)	Adsorbent dosage (g L^{-1})	References
AMSD	70	33.73	30	0.2	[21]
Phoenix *Dactylifera* seeds	20	61.72	120	0.6	[22]
Natural Serpentine	100	15.36	180	0.2	[37]
Soil	50	2.230	40	2.5	[39]
Activated *Moringo oleifera* seed coat	10	1.861	90	0.1	[41]
Solanum tubersum	50	6.9	50	0.8	[42]
Pisum sativum	50	16.4	35	0.6	[42]
Limonia acidissima	50	60.22	120	0.5	[43]
Aloe-vera leaves shell	100	91	20	1.0	[44]
Cedrus deodara sawdust	100	182.5	20	0.25	Present work

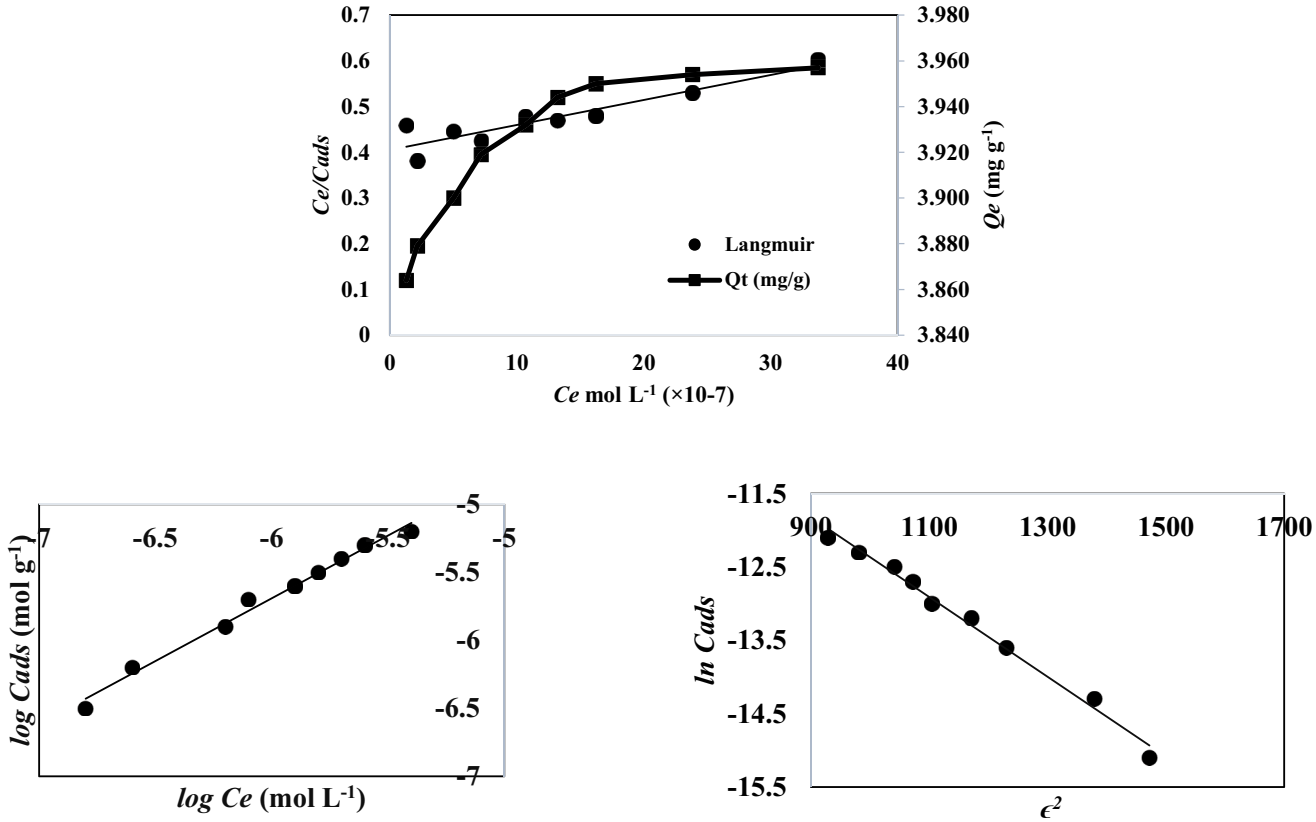

Fig. 10. Isotherm plots for aqueous removal of Congo red over saw dust of *C. deodara.*

where R is the general gas constant, T is the absolute temperature in Kelvin and C_e is the concentration of dye adsorb at time of equilibrium (mol g^{-1}).

The linearized form of the above D–R isothermal equation [36]:

$$\ln C_{ads} = \ln C_m - \beta\varepsilon^{-2} \tag{15}$$

Through the value of β the mean energy of the adsorption process (E_s) can be calculated as follows [35]:

$$E_s = \frac{1}{\left(-2\beta\right)^{1/2}} \tag{16}$$

where E_s is the mean free energy transfer of one mole of dye to the surface of adsorbent (*C. deodara* saw).

By using the linear form of the D–R isotherm equation a straight-line plot between $\ln C_{ads}$ vs. ε^2 for the adsorption of Congo red over sawdust of *C. deodara* obtained and displayed in Fig. 10c. The slope and intercept values used for determining the E_s and β constants values are given in Table 2. The value of β (0.0054) used to calculate the adsorption energy (E_s) which is 7.44 kJ mol^{-1}. Higher the value of free sorption reveals the stronger bonding between adsorbate molecules and adsorbent surfaces. The values of regression R^2 and SSE were predicting that the D–R isotherm was showing the best fitness towards the experimental data. The value of R^2 and SSE are 0.9964 and 0.004 for D–R isothermal model.

3.6. Thermodynamics of adsorption

Heat changes in a system or state of a system can be defined by some state functions including Gibbs free energy (Δ*G*), entropy (Δ*S*), and enthalpy (Δ*H*). And in the determination of these parameters will show the nature of the adsorption process either it is exothermic or endothermic in nature. All these parameters of thermodynamics can be determined by the given expression [35]:

$$\ln K_c = \left(\frac{\Delta S}{R}\right) - \left(\frac{\Delta H}{\mathrm{RT}}\right) \tag{17}$$

Δ*S* is entropy (account for disturbance of system) Δ*H* is enthalpy or total heat content of the system, T stands for temperature in Kelvin, K_c is the equilibrium constant.

$$K_c = \frac{C_a}{C_e} \tag{18}$$

where C_a and C_e are the equilibrium constants, the amount of dye adsorb on adsorbent (mol L^{-1}) at equilibrium and equilibrium concentration of dye in solution (mol L^{-1}), respectively. If adsorption is an exothermic process then there will be negative values for the Gibbs free energy, entropy, and enthalpy and the relation between these parameters is as follows [38]:

$$\Delta G^\circ = \Delta H^\circ - T\Delta S^\circ \tag{19}$$

The negative value of enthalpy and entropy generally shows the exothermic nature of the reaction. So, the present adsorption process represented inverse relation with the temperature, as the temperature increases, it will decrease the adsorption of Congo red on the *C. deodara* saw surface and vice versa [39]. The plot between $\ln K_c$ vs. $1/T$ for adsorption of Congo red dye over sawdust of *C. deodara* can be demonstrated by Fig. 11. The values for the adsorption enthalpy ($\Delta H°$) and adsorption entropy ($\Delta S°$) were calculated by the slope and intercept from the plot between $\ln K_c$ vs. $1/T$. The values for Gibb's free energy ($\Delta G°$) for the adsorption of Congo red over sawdust were calculated by using the above relation-19. Values for all thermodynamics parameters are represented in Table 4. Decrease in value of $\Delta G°$ with rise in temperature represents the decrease in feasibility and adsorption at higher temperature. Further, the negative value for $\Delta G°$ revealed that the process was spontaneous in nature. The positive value for enthalpy $\Delta H°$ predicts that the adsorption of Congo red dye was an endothermic mechanism. Likewise, the positive value for entropy $\Delta S°$ was exhibit an increase in randomness at the interface of adsorbent–adsorbate during the adsorption of Congo red over sawdust of *C. deodara*.

Table 4
Parameters of thermodynamics

T (K)	Q (mg L^{-1})	ΔG (kJ/mol)	ΔH (kJ/mol)	ΔS (J/mol K)
273	9.74	–5.519		0.091
283	7.82	–6.115		0.067
293	6.55	–6.588		0.089
303	5.01	–7.293	19.422	0.088
313	5.06	–7.839		0.087
323	3.00	–8.617		0.087
333	2.28	–9.315		0.086
343	1.94	–9.724		0.085

Table 5
Results of tap water solution

Dye	%age removal	Conditions
Congo red	94%	100 mg L^{-1} dye conc., 20 min shaking time at 7.0 pH

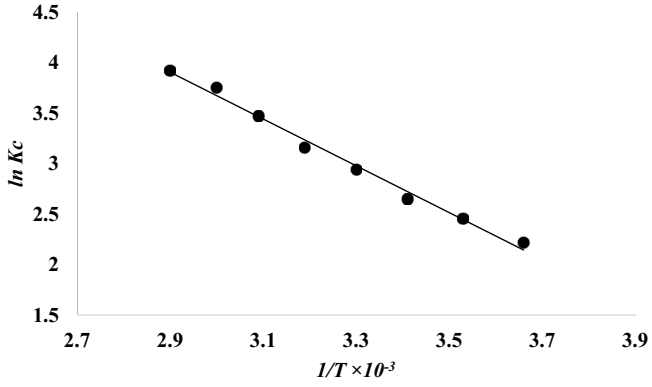

Fig. 11. Thermodynamics of adsorption.

3.7. Applicability of developed procedure

The same procedure with optimized conditions was applied to the real sample of tap water solution of Congo red dye was investigated over *C. deodara* saw. The maximum adsorption of Congo red dye solution of tap water was 94%. The data for the percentage adsorption of Congo red is given in Table 5. Results are a clear indication that the sawdust of *C. deodara* can be potentially used for the removal of Congo red dye. This developed procedure can be applied for the removal of Congo red dye from the wastewater or effluents.

4. Conclusion

In this research article, the batch sorption study of Congo red dye from its aqueous solution over sawdust of *C. deodara* was carried out in detail. The percentage removal of Congo red dye was increased with the impact of several parameters: temperature, adsorbent weight, pH, and contact time while it was decreased with initial dye concentration. The kinetic study of sorption revealed that the experimental data for adsorption of Congo red dye over sawdust of *C. deodara* was best fitted with pseudo-second-order kinetic model based on values and D–R isothermal expression based on SSE (0.9962, 0.004) values. The adsorbent surface was characterized by FT-IR and SEM analysis. Thermodynamic studies revealed that Congo red dye adsorption over sawdust of *C. deodara* is an endothermic spontaneous process in nature. The present experimental analysis concluded that *C. deodara* saw can be used efficiently as an alternative adsorbent to remove Congo red dye from aqueous media.

References

[1] A. Mittal, J. Mittal, A. Malviya, V. Gupta, Adsorptive removal of hazardous anionic dye "Congo red" from wastewater using waste materials and recovery by desorption, J. Colloid Interface Sci., 340 (2009) 16–26, doi: 10.1016/j.jcis.2009.08.019.
[2] M.A. Salleh, D.K. Mahmoud, W.A. Karim, A. Idris, Cationic and anionic dye adsorption by agricultural solid wastes: a comprehensive review, Desalination, 280 (2011) 1–13, doi: 10.1016/j.desal.2011.07.019.
[3] M. Khadhraoui, H. Trabelsi, M. Ksibi, S. Bouguerra, B. Elleuch, Discoloration and detoxification of a Congo red dye solution by means of ozone treatment for a possible water reuse, J. Hazard. Mater., 161 (2009) 974–981, doi: 10.1016/j.jhazmat.2008.04.060.
[4] T.W. Seo, K.L. Ch, Removal of dye by adsorption: a review, Int. J. Appl. Eng. Res., ISSN 0973–4562, 1 (2016) 2675–2679.
[5] Z.L. Yaneva, N.V. Georgieva, Insight into Congo red adsorption on agro-industrial materials-spectral, equilibrium, kinetics, thermodynamics, dynamics and desorption studies, a review, Int. Rev. Chem. Eng., 4 (2012) 127–146.
[6] A. Tor, Y. Cengeloglu, Removal of Congo red from aqueous solution by adsorption onto acid activated red mud, J. Hazard. Mater., 138 (2006) 409–415, doi: 10.1016/j.jhazmat.2006.04.063.
[7] M. Yagub, T. Sen, S. Afroze, H. Ang, Dye and its removal from aqueous solution by adsorption: a review, Adv. Colloid Interface Sci., 209 (2014) 172–184, doi: 10.1016/j.cis.2014.04.002.

[8] M. Haque, M. Haque, M. Mosharaf, P. Marcus, Novel bacterial biofilm consortia that degrade and detoxify the carcinogenic diazo dye Congo red, Arch. Microb., 203 (2020) 643–654, doi: 10.1007/s00203-020-02044-1.
[9] V. Karthik, K. Saravanan, P. Bharathi, V. Dharanya, C. Meiaraj, An overview of treatments for the removal of textile dyes, J. Chem. Pharm. Sci., 7 (2014) 301–307.
[10] N. Shah, J. Khan, M. Sayed, Z. Khan, J. Iqbal, S. Arshad, M. Junaid, H. Khan, Synergistic effects of H_2O_2 and $S_2O_8^{2-}$ in the gamma radiation induced degradation of Congo-red dye: kinetics and toxicities evaluation, Sep. Purif. Technol., 233 (2020) 115966, doi: 10.1016/j.seppur.2019.115966.
[11] A. Wahabou, A. Ntieche Rahman, K. Daoud, A. Paltahe, Adsorption of Congo red on activated carbon modified by plasma, Int. J. Eng. Sci. Res., 5 (2017) 30–43, ISSN: 2347-653.
[12] T. Robinson, G. Mcmullan, R. Marchant, P. Nigam, Remediation of dyes in textile effluent: a critical review on current treatment technologies with a proposed alternative, Bioresour. Technol., 77 (2001) 247–255, doi: 10.1016/s0960-8524(00)00080-8.
[13] M. Kharub, Use of various technologies, methods and adsorbent for the removal of dye, J. Environ. Res. Dev., 6 (2012) 879–883.
[14] M. Doğan, Y. Özdemir, M. Alkan, Adsorption kinetics and mechanism of cationic methyl violet and methylene blue dyes onto sepiolite, Dye Pigm., 75 (2007) 701–713, doi: 10.1016/j.dyepig.2006.07.023.
[15] L.B. Lim, N. Priyantha, K.J. Mek, N.A. Zaidi, Application of *Momordica charantia* (bitter gourd) waste for the removal of malachite green dye from aqueous solution, Desal. Water Treat., 154 (2019) 385–394, doi: 10.5004/dwt.2019.24115.
[16] L.B. Lim, N. Priyantha, S.A. Latip, Y. Lu, A.H. Mahadi, Converting *Hylocereus undatus* (white dragon fruit) peel waste into a useful potential adsorbent for the removal of toxic Congo red dye, Desal. Water Treat., 185 (2020) 307–317, doi: 10.5004/dwt.2020.25390.
[17] R.P. Mohubedu, P.N. Diagboya, C.Y. Abasi, E.D. Dikio, F. Mtunzi, Magnetic valorization of biomass and biochar of a typical plant nuisance for toxic metals contaminated water treatment, J. Cleaner Prod., 209 (2019) 1016–1024, doi: 10.1016/j.jclepro.2018.10.215.
[18] H. Zhu, R. Jiang, L. Xiao, Adsorption of an anionic azo dye by chitosan/kaolin/γ-Fe_2O_3 composites. Appl. Clay Sci., 48 (2010) 522–526, doi: 10.1016/j.clay.2010.02.003.
[19] M.R. Kooh, M.K. Dahri, L.B. Lim, L.H. Lim, Batch adsorption studies on the removal of Acid Blue 25 from aqueous solution using *Azolla pinnata* and soya bean waste, Arabian J. Sci. Eng., 41 (2015) 2453–2464, doi: 10.1007/s13369-015-1877-5.
[20] M.K. Dahri, L.B. Lim, C.C. Mei, Cempedak durian as a potential biosorbent for the removal of Brilliant Green dye from aqueous solution: equilibrium, thermodynamics and kinetics studies, Environ. Monit. Assess., 187 (2015), doi: 10.1007/s10661-015-4768-z.
[21] P. Patil, Y. Marathe, V. Shrivastava, Evaluation of the adsorption kinetics and equilibrium for the potential removal of Congo red dye from aqueous medium by using a biosorbent, Br. J. Appl. Sci. Technol., 6 (2015) 557–573, doi: 10.9734/bjast/2015/12590.
[22] D. Pathania, A. Sharma, Z. Siddiqi, Removal of Congo red dye from aqueous system using *Phoenix dactylifera* seeds, J. Mol. Liq., 219 (2016) 359–367, doi: 10.1016/j.molliq.2016.03.020.
[23] N.B. Swan, M.A. Zaini, Adsorption of Malachite Green and Congo red dyes from water: recent progress and future outlook, Ecol. Chem. Eng. S, 26 (2019) 119–132, doi: 10.1515/eces-2019-0009.
[24] F.A. Pavan, S.L. Dias, E.C. Lima, E.V. Benvenutti, Removal of Congo red from aqueous solution by anilinepropylsilica xerogel, Dye Pigm., 76 (2008) 64–69, doi: 10.1016/j.dyepig.2006.08.027.
[25] A.R. Omran, M.A. Baiee, S.A. Juda, J.M. Salman, A.F. AlKaim, Removal of Congo red dye from aqueous solution using a new adsorbent surface developed from aquatic plant (Phragmitesaustralis), Int. J. Chem. Technol. Res., ISSN: 0974-4290, 9 (2016) 334–342, 201.
[26] L. Wang, A. Wang, Adsorption behaviors of Congo red on the N,O-carboxymethyl-chitosan/montmorillonite nanocomposite, Chem. Eng. J., 143 (2008) 43–50, doi: 10.1016/j.cej.2007.12.007.
[27] T.A. Ojo, A.T. Ojedokun, O.S. Bello, Functionalization of powdered walnut shell with orthophosphoric acid for Congo red dye removal, Part. Sci. Technol., 37 (2017) 74–85, doi: 10.1080/02726351.2017.1340914.
[28] S. Das, S. Singh, S. Garg, Evaluation of wheat bran as a biosorbent for potential mitigation of dye pollution in industrial waste waters, Orient. J. Chem., 35 (2019) 1565–1573, doi: 10.13005/ojc/350514.
[29] J.O. Nnaemeka, K.E Conrad, O Synthia, Adsorptive removal of crystal violet using agriculture waste: equilibrium, kinetics and thermodynamics studies, Am. J. Eng. Res., 8 (2019) 38–51.
[30] X. Yuan, F. Zhou, R. Man, J. Huang, Dendritic post-cross-linked resin for the adsorption of crystal violet from aqueous solution, J. Chem. Therm., 130 (2019) 235–242, doi: 10.1016/j.jct.2018.09.030
[31] S. Zafar, M.I. Khan, M. Khraisheh, S. Shahida, T. Javed, M.L. Mirza, N. Khalid, Use of rice husk as an effective sorbent for the removal of cerium ions from aqueous solution: kinetic, equilibrium and thermodynamic studies, Desal. Water Treat., 150 (2019) 124–135, doi: 10.5004/dwt.2019.23724.
[32] S. Ata, M.I. Din, A. Rasool, I. Qasim, I.U. Mohsin, Equilibrium, thermodynamics, and kinetic sorption studies for the removal of coomassie Brilliant Blue on Wheat Bran as a low-cost adsorbent, J. Anal. Methods Chem., (2012) 1–8, doi: 10.1155/2012/405980.
[33] S. Boumchita, A. Lahrichi, Y. Benjelloun, S. Lairini, V. Nenov, F. Zerrouq, Application of peanut shell as a low-cost adsorbent for the removal of anionic dye from aqueous solutions, J. Mater. Environ. Sci., 8 (2017) 2353–2364.
[34] A. Mahapatra, B. Mishra, G. Hota, Adsorptive removal of Congo red dye from wastewater by mixed iron oxide–alumina nanocomposites, Cer. Intern., 39 (2013) 5443–5451, doi:10.1016/j.ceramint.2012.12.052.
[35] M.S. Abbas, R. Ahmad, Equilibrium, kinetic and thermodynamic study of acid yellow-34 adsorption onto *Cedrus deodara* sawdust, Desal. Water Treat., 57 (2015) 18175–18181, doi: 10.1080/19443994.2015.1089199.
[36] T. Javed, N. Khalid, M.L. Mirza, Removal of lead ions from aqueous solutions by low-rank Pakistani coal, Desal. Water Treat., 81 (2017) 133–142, doi: 10.5004/dwt.2017.21095.
[37] M. Shaban, M.R. Abukhadra, A.A. Khan, B.M. Jibali, Removal of Congo red, methylene blue and Cr(VI) ions from water using natural serpentine, J. Taiwan Inst. Chem. Eng., 82 (2018) 102–116, doi: 10.1016/j.jtice.2017.10.023.
[38] M. Purkait, A. Maiti, S. Dasgupta, S. De, Removal of Congo red using activated carbon and its regeneration, J. Hazard. Mater., 145 (2007) 287–295, doi: 10.1016/j.jhazmat.2006.11.021.
[39] C. Smaranda, M. Gavrilescu, D. Bulgariu, Studies on sorption of Congo red from aqueous solution onto soil, Int. J. Environ. Res., 5 (2011) 177–188, Winter 2011 ISSN: 1735–6865.
[40] S. Omidi, A. Kakanejadifard, Eco-friendly synthesis of graphene–chitosan composite hydrogel as efficient adsorbent for Congo red, RSC Adv., 8 (2018) 12179–12189, doi: 10.1039/c8ra00510a.
[41] J.M. Jabar, Y.A. Odusote, K.A. Alabi, I.B. Ahmed, Kinetics and mechanisms of congo-red dye removal from aqueous solution using activated *Moringa oleifera* seed coat as adsorbent, Appl. Water Sci., 10 (2020), doi: 10.1007/s13201-020-01221-3.
[42] R. Rehman, I. Manzoor, L. Mitu, Isothermal study of Congo red dye biosorptive removal from water by *Solanum tuberosum* and *Pisum sativum* peels in economical way, Bull. Chem. Soc. Earth, 32 (2018) 213, doi: 10.4314/bcse.v32i2.3.
[43] V. Yadav, D. Tiwari, M. Bhagat, Removal of Congo red dye from aqueous solution by using *Limonia acidissima* shell as adsorbent, Asian J. Chem., 30 (2018) 2765–2770, doi: 10.14233/ajchem.2018.21611.
[44] Y.O. Khaniabadi, M.J. Mohammadi, M. Shegerd, S Sadeghi, H. Basiri, Removal of Congo red dye from aqueous solutions by a low-cost adsorbent: activated carbon prepared from *Aloe vera* leaves shell, Environ. Health Eng. Manage., 4 (2016) 29–35, doi:10.15171/ehem.2017.05.